doi: 10.12029/gc20190616

谢纪海, 胡正祥,毛新武, 孔令耀, 杨青雄, 杨成, 郭盼. 2019. 鄂北大洪山晋宁期MORB-like玄武岩的识别与洋内俯冲作用[J]. 中国地质, 46(6): 1496-1511.

Xie Jihai, Hu Zhengxiang, Mao Xinwu, Kong Lingyao, Yang Qingxiong, Yang Cheng, Guo Pan. 2019. The discrimination of Jinningian MORB-like basalt and intra-oceanic subduction in the Dahongshan area, Northern Hubei[J]. Geology in China, 46(6): 1496-1511(in Chinese with English abstract).

鄂北大洪山晋宁期MORB-like玄武岩的识别与洋内俯冲作用

谢纪海[1], 胡正祥[2], 毛新武[2], 孔令耀[2], 杨青雄[2], 杨成[2], 郭盼[2]

(1. 武汉测绘研究院,湖北 武汉 430034;2. 湖北省地质调查院,湖北 武汉 430034)

提要:鄂北随州大洪山地区出露大量镁铁质岩(如:辉长岩、辉绿岩、(枕状)玄武岩),它们主要以岩块的形式构造混杂在一套碎屑岩中,表现为典型造山带基质-岩块混杂的特征。大洪山镁铁质岩为拉斑玄武岩系列岩石组合,地球化学方面,不相容元素Rb、Ba、K、Th、U富集,高场强元素Nb、Ta亏损,表现为岛弧玄武岩的特点,而平坦的稀土配分模式(ΣLREE/ΣHREE=1.41~4.48, La_N/Yb_N=0.76~4.79),Zr/Y=2.65~5.38,Ti/V=29.19~54.97,又可与洋中脊玄武岩对比。因此,我们推测大洪山镁铁质岩属于MORB-like玄武岩(或前弧玄武岩)类岩石组合,其形成于洋内初始俯冲环境,成岩岩浆由俯冲洋板片脱水交代亏损洋中脊地幔减压熔融产生。通过LA-ICP-MS锆石U-Pb测年,分别获得南风垭、绿林寨玄武岩(816.6±7.6) Ma (MSWD=0.47)、(813.1±4.8) Ma (MSWD=0.37)的成岩年龄,结合已经取得的杨家棚辉长岩947 Ma、厂河枕状玄武岩824 Ma、绿林辉绿岩820 Ma的年龄结果,说明大洪山地区的这套前弧镁铁质岩组合大致形成于817~947 Ma,它们可能是多阶段洋内俯冲的产物。大洪山地区这套前弧镁铁质岩的厘定说明扬子地块与桐柏-大别地块之间晋宁期发生过一定规模的洋内-洋陆俯冲和造山运动,二者可能曾在青白口纪晚期拼合到一起。

关 键 词:鄂北大洪山;晋宁期;地球化学;锆石U-Pb测年;MORB-like玄武岩;洋内弧;俯冲造山作用;地质调查工程

中图分类号:P588.145;P542.4 **文献标志码:**A **文章编号:**1000-3657(2019)06-1496-16

The discrimination of Jinningian MORB-like basalt and intra-oceanic subduction in the Dahongshan area, Northern Hubei

XIE Jihai[1], HU Zhengxiang[2], MAO Xinwu[2], KONG Lingyao[2], YANG Qingxiong[2], YANG Cheng[2] , GUO Pan[2]

(1. *Wuhan Geomatics Institute, Wuhan* 430034*, Hubei, China;* 2. *Hubei Geological Survey, Wuhan* 430034*, Hubei, China*)

收稿日期:2018-02-13;**改回日期:**2019-03-25

基金项目:湖北省地质局科技项目"扬子陆块北缘(湖北段)基底组成、结构、演化及成矿作用研究"(KJ2019-2)和中国地质调查局项目"湖北1:5万长岗店、均川、客店坡、古城畈、三阳店幅区域地质调查"(12120113012800)联合资助。

作者简介:谢纪海, 男, 1976年生, 高级工程师, 水文地质工程地质专业, 从事城市地质调查、地质灾害防治、岩土工程等技术及管理工作;E-mail:51344552@qq.com。

通讯作者:胡正祥,男,1963年生,教授级高级工程师,地质矿产勘查专业,从事地质矿产调查与技术管理工作;E-mail: 1113153933@qq.com。

Abstract: There are numerous mafic rocks e.g., gabbro, diabase, basalt, pillow basalt, fumarolic-amygdaloidal basalt, in the Dahongshan area, Suizhou City, northern Hubei Province. They are mainly in the form of block structurally mixed in a set of clastic rock, characterized by mélange of exotic blocks and matrix strata, suggesting a typical orogenic belt. The mafic rocks from Dahongshan area show the features of tholeiite series, and are geochemically enriched in incompatible elements such as Rb, Ba, K, Th and U and depleted in high field strength elements such as Nb and Ta, similar to features of island arc basalts. Nevertheless, the features of flat REE patterns (ΣLREE/ΣHREE=1.41-4.48, La_N/Yb_N=0.76-4.79, Zr/Y=2.65-5.38 and Ti/V=29.19-54.97) are the same as features of mid-ocean ridge basalt. Therefore, the geochemical signatures and regional geological characteristics show that these mafic rocks should be part of MORB-like/ fore-arc basalts, formed along intra-ocean arc where the subduction-initiation happened. Their parent magma was produced by the nascent depleted MORB mantle and interacted with the contribution of fluids from the slab sinking plate with decompression melting. The basalts from Nanfengya and Lulinzhai yielded LA-ICP-MS U-Pb zircon ages of (816.6±7.6) Ma (MSWD=0.47) and (813.1±4.8) Ma (MSWD=0.37) respectively, interpreted as their crystallization age. Combined with the previous research results of gabbro in Yangjiapeng (947 Ma), pillow basalt in Changhe (824 Ma), and diabase in Luling (820 Ma), it is held that mass mafic rocks were formed in Jinningian period (817-947 Ma) in the Dahongshan area. They may be the products of multi-stage intra-ocean subduction. The discrimination of Jinningian ore-arc/ MORB-like basalt in the Dahongshan suggests that it experienced a certain scale of ocean-ocean to ocean-continent subduction and orogeny between Yangtze block and Tongbai-Dabie block in Jinningian period, and the two blocks might have been aggregated together in late Qingbaikou period.

Key words: Dahongshan area; northern Hubei Province; Jinningian; geochemistry; zircons U-Pb dating; MORB-like basalt; intra-ocean arc; subduction orogeny; geological survey engineering

About the first author: XIE Jihai, male, born in 1976, senior engineer, majors in hydrogeology and engineering geology, engages in urban geological survey, prevention and cure of geological hazard, geotechnical engineering and technical management; E-mail: 51344552@qq.com.

About the corresponding author: HU Zhengxiang, male, born in 1963, professor, majors in geological and mineral exploration, engages in geological and mineral investigation and technical management; E-mail: 1113153933@qq.com.

Fund support: Supported by Hubei Geological Bureau Science and Technology Project (No. KJ2019-2) and China Geological Survey Program (No. 12120113012800).

1 引　言

鄂北随南大洪山地区位于扬子地块与桐柏—大别地块之间，是研究扬子地块与桐柏—大别地块拼合、造山运动的关键地区之一(任纪舜等, 2017)。早期的1:20万、1:5万区域地质调查认为大洪山地区主要由中元古代打鼓石群稳定陆缘沉积和角度不整合之上的花山群碎屑-火山岩组成[1][2]。在后来的研究中，董云鹏对花山群进行解体，将北部以玄武岩为主的基性火山岩定义为构造侵位的蛇绿混杂岩，称其为“花山蛇绿构造混杂岩”，并根据卷入地层的时代推测花山地区存在海西—早印支期初始小洋盆，该洋盆于中三叠世闭合(董云鹏等, 1998, 1999; Dong et al., 1999)，并且长期以来，多数学者认为“花山蛇绿构造混杂岩”代表的缝合带向西与勉略缝合带相连(Lai et al., 1999; 董云鹏等, 2003; 张国伟等, 2003, 2004; Dong et al., 2015)。然而部分学者对混杂带内岩浆岩进行同位素年代学研究，不同测试方法获得的年龄结果差异较大(石玉若等, 2003, 2005a, b; 张宗清等, 2006;Shi et al., 2007)，使得随南花山地区这套“混杂岩”一直缺少精确、统一的同位素年代学证据。

笔者近年对大洪山地区调查研究发现(图1)，大洪山地区主要由沿土门—小阜—园潭一线的岛弧侵入岩、火山-碎屑岩及南侧的增生杂岩组成，并且分别在岩浆弧和杂岩中获得大量青白口纪的锆石U-Pb同位素年龄，并初步推测杂岩中的镁铁质岩岩块为洋中脊蛇绿岩套的基性端元残块，大洪山地区可能存在一条不同于勉略带的晋宁期缝合带(胡正祥等, 2015a, b)。然而此认识与前人“勉略带东延”的观点有着较大的差异，因此需要更多可靠的地质资料和系统的分析研究来证实大洪山地区

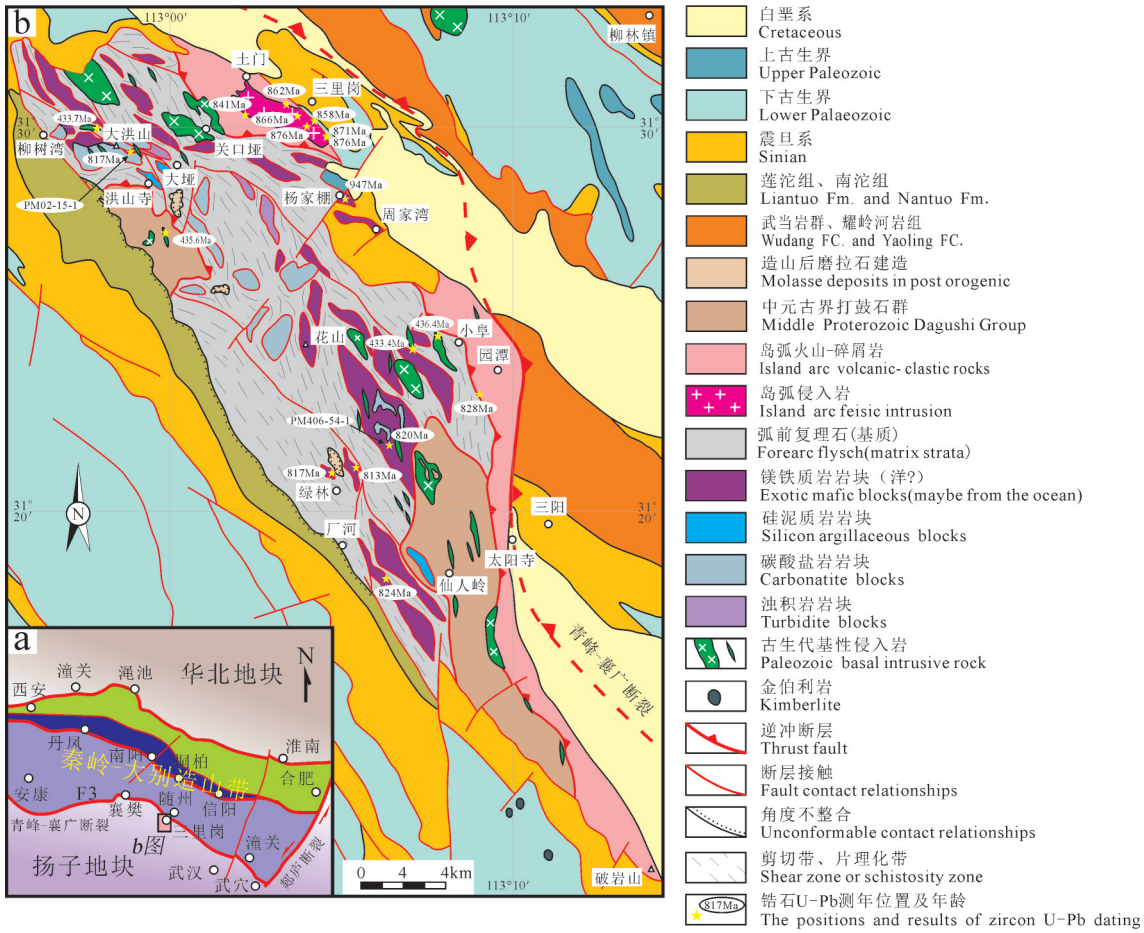

图1 大洪山地区地质简图

（图中相关测年位置及数据参考Shi et al., 2007; 胡正祥等, 2015a, 2017; 廖明芳等, 2016; Xu et al., 2016; 陈超等, 2017a, b, 2018 ）

Fig.1 The geological sketch map of Dahongshan area

（Locations and results of zircons U-Pb dating in the map after Shi et al., 2007; Hu Zhengxiang et al., 2015a, 2017; Liao Mingfang et al., 2016; Xu et al., 2016; Chen Chao et al., 2017a, b, 2018）

物质组合的真实形成环境和形成时代。本文以大洪山地区前南华纪物质建造为研究对象，重点分析其野外产出、地球化学及年代学特点，旨在查明大洪山晋宁期缝合带主要物质组成及成因，为探讨新元古代扬子北缘形成演化过程提供依据。

2 地质背景及岩石学特征

研究区位于秦岭造山带东段、扬子地块与南秦岭（桐柏—大别）地块的结合部位，北界为勉略—青峰—襄（樊）广（济）区域性深大断裂，南侧被南华系莲沱组角度不整合覆盖。区内主要出露一套中元古代—青白口纪的物质建造，少量震旦系、古生界、白垩系在后期构造运动中呈断块混入其中，平面上整体呈“透镜状”分别于北西和南东向尖灭（图1）。结合前人的研究成果和最新野外地质调查资料，在这长、宽小于25 km×20 km区域内，笔者系统鉴别出了中元古代稳定陆缘沉积——打鼓石群、青白口纪活动大陆边缘岛弧火山岩—侵入岩组合和代表洋盆消亡的俯冲增生杂岩等三套主要物质(胡正祥等, 2015a)。南侧打鼓石群为一套以白云岩、砂岩、(泥)板岩为主的稳定大陆边缘沉积，具有较为稳定的层序和相对较弱的变形特征，其中的凝灰岩夹层SHRIMP锆石U-Pb年龄为约12 Ga(李怀坤等, 2016)。北侧主体为一套以基性为主，夹安山岩、英安岩、流纹岩及少量粉砂岩的岛弧火山-碎屑岩(Dong et al., 2006；胡正祥等, 2017)，笔者已分别在土门和仓头垭酸性火山岩中获得841 Ma、828 Ma的LA-ICP-MS锆石U-Pb年龄(胡正祥等, 2015a,

2017);其次,三里岗岩体也具有岛弧中—酸性侵入岩的特点,其形成时间应为858~876 Ma(Shi et al., 2007; 廖明芳等, 2016; Xu et al., 2016)。在稳定大陆边缘沉积和岩浆弧之间,主体为一套砂岩、板岩构成的碎屑岩组合,具有较强的变形特征,主要发育一组NNE倾向紧闭同斜(局部倒转)褶皱和逆冲断层(图2a),共同指示SSW向的逆冲推覆作用。这套碎屑岩中发育大量岩性、规模、形态各异的岩块,包括砾岩岩块、硅泥岩岩块、白云岩岩块、辉长(绿)岩岩块、玄武岩岩块等,它们以构造混杂的形式呈断块夹在碎屑岩中(图2b、d),显示出典型造山带俯冲增生杂岩的特点。前期笔者曾报道绿林镇一带的角砾状玄武岩,其具有碱性、轻稀土元素和不相容元素强烈富集的洋岛玄武岩的特点,且用LA-ICP-MS法获得817 Ma的成岩年龄,推测为洋岛/海山环境下的产物(陈超等, 2017a)。除此之外,杂岩中还存在大量的镁铁质岩岩块(包括辉长岩、辉绿岩、玄武岩岩块),其岩性组合、岩石系列均与绿林洋岛玄武岩存在一定差异,本文主要讨论其形成环境、时代,镁铁质岩岩块具有如下岩石学特征。

辉长岩:灰绿色,变辉长结构,块状构造,主要由斜长石(60%)和辉石(35%)组成,二者自形程度相近,均呈半自形板状,粒度较大,0.8~1.5mm不等,基性斜长石发生较强蚀变,大部分被黏土矿物和钠黝帘石取代,仅保留其晶体轮廓,辉石有一定程度的绿泥石化、蛇纹石化,局部可见角闪石的反应边,岩石整体有较强的钛-磁铁矿化(图2c,图3a)。

辉绿岩:灰绿色,变辉绿结构,块状构造,主要由斜长石(65%)和辉石(25%)组成,斜长石呈板条状构成架状,表面绢云母化、碳酸盐化强烈,部分保留完整晶形,辉石分布于斜长石矿物间隙中,呈他形粒状,几乎全部被绿泥石、方解石微粒集合体取代,岩石中铁质矿物(10%)较多,以黄铁矿为主,可能有部分磁铁矿或钛铁矿(图2e,图3b)。

气孔-杏仁状玄武岩:灰绿色、浅绿色,变间粒结构,气孔、杏仁构造,块状构造,主要由斜长石(50%)和基性玻璃质成分(40%)组成,含少量钛磁铁矿(8%)和方解石(2%),斜长石呈半自形板条状,粒径0.1~0. 3mm,部分斜长石发生黏土化,基性玻璃基本被鳞片状绿泥石取代,气孔内主要充填方解石(图2f,图3c)。

枕状玄武岩:露头尺度上岩石暗绿色,隐晶质结构,枕状构造发育,单个"枕"大小15~40 cm不等,排列紧密,表现为海相火山岩的特点;镜下主要发育玻基交织结构,局部可见气孔、杏仁构造,主要由半自形长条状基性斜长石(62%)和他形粒状角闪石(25)组成,含少量玻璃质成分(10%)和磁铁矿(3%)(图2g、h,图3d)。

3　分析方法

全岩主量元素、微量元素和稀土元素分析均在武汉综合岩矿测试中心化学分析研究室完成。主量元素SiO_2、TiO_2、Al_2O_3、TFe_2O_3、MnO、MgO、CaO、Na_2O、K_2O、P_2O_5采用X荧光光谱法(XRF)在X荧光光谱仪(XRF-1800)上测定,而FeO则是通过湿化学分析方法获得,微量元素和稀土元素分析采用电感耦合等离子质谱法(ICP-MS)在电感耦合等离子体质谱仪(X2)上测定。具体实验方法和步骤参考马天芳等 (2011),分析结果见表1,采用Geokit软件对实验数据的分析、处理(路远发, 2004)。

两件锆石测年玄武岩样品PM02-15-1、PM406-54-1分别采自大洪山顶附近南风垭(GPS:112°59′18.796″E,31°28′53.214″N)和绿林寨景区内的公路边(GPS:113°6′36.908″E,31°21′15.246″N),样品重量均大于25 kg。单矿物锆石挑选在廊坊市诚信地质服务有限公司完成,透射光、反射光和阴极发光图像(CL)的拍摄在北京锆年领航科技有限公司完成。LA-ICP-MS锆石U-Th-Pb同位素和微量元素微区分析在湖北省地质试验测试中心完成,测试仪器采用美国Coherent Inc公司生产的GeoLasPro全自动版193 nm ArF准分子激光剥蚀系统(LA)和美国Agilent公司生产的7700X型电感耦合等离子质谱仪(ICP-MS)联用构成的激光剥蚀电感耦合等离子体质谱分析系统(LA-ICP-MS),激光束斑直径为32 μm,用He作为剥蚀物质的载气,哈佛大学标准锆石91500作为外标,^{29}Si作为内标,GJ-1或者Plešovic为监控标样,具体操作详见周亮亮等, (2017),采用ICPMSDataCal(V7.2)软件对同位素比值数据进行处理(Liu et al., 2008),对实验测得的数据用ISOPLOT程序进行谐和图的绘制以及

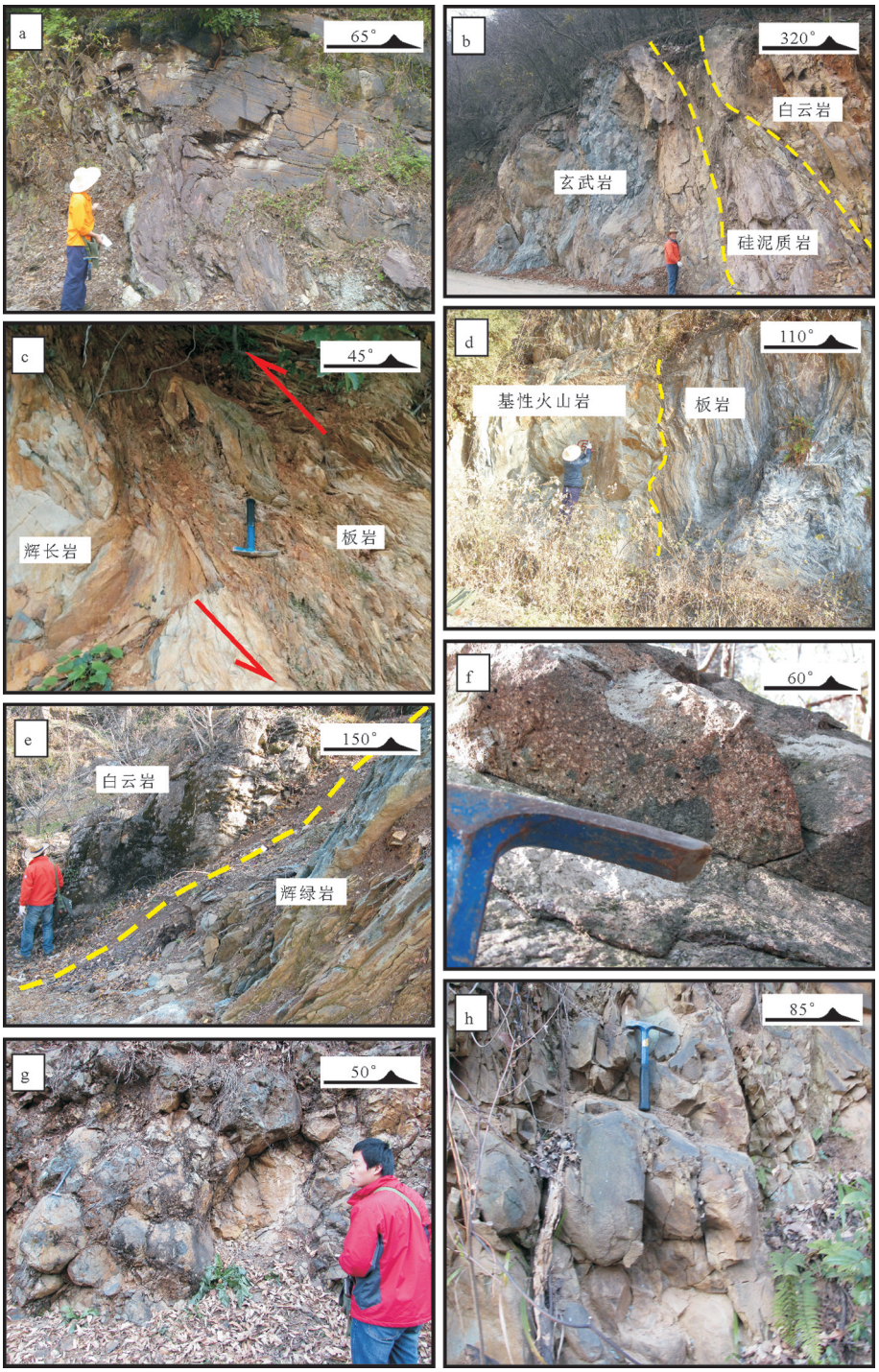

图2 大洪山俯冲增生杂岩及镁铁质岩野外特征

a—厂河砂岩中发育同斜倒转褶皱;b—南风垭玄武岩、紫红色硅泥质岩、白云岩混杂;c—关口垭粉砂质板岩逆冲到辉长岩之上,二者接触面上发育构造透镜体;d—关口垭绢云母板岩中夹基性火山岩岩块;e—罗家咀硅质条带白云岩中的辉绿岩脉,辉绿岩发生强片理化;f—罗家咀北气孔-杏仁状玄武岩;g—厂河枕状玄武岩;h—姚家冲西枕状玄武岩

Fig.2 Field photos of the subduction accretionary complex and mafic rocks in Dahongshan

a-Synclinal overturned fold developed in the sandstone in Changhe; b-Mélange in Nanfengya composed of basalt, fuchsia siliceous argillaceous rock and dolomite; c- Silty argillaceous thrust up to the gabbro, and tectonic lenses developed between them in the Guankouya; d-Basic volcanic rock mass mixed in the sericite slate in Guankouya; e-Strong foliated doleritic vein developed in the siliceous band dolomite in Luojiaju; f-Amygdaloidal basalts outcropped in the north of Luojiaju; g-Pillow basalts outcrop in Changhe; h-Pillow basalts outcrop in the west of Yaojiachong

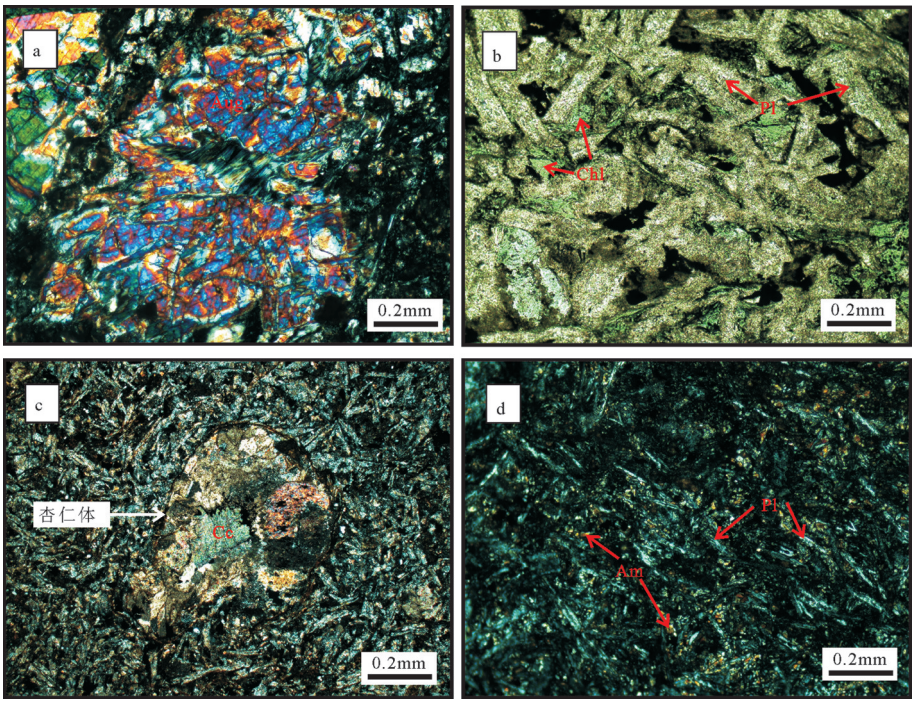

图3 大洪山镁铁质岩镜下特征

a—关口垭辉长岩中辉石局部蚀变成透闪石、绿泥石，斜长石基本被粘土矿物交代(+)；b—罗家咀辉绿岩中的辉绿结构，辉石基本被绿泥石取代(−)；c—厂河东气孔-杏仁状玄武岩中的杏仁构造，充填物主要为方解石(+)；d—厂河枕状玄武岩间粒结构(+)；Am—角闪石，Aug—普通辉石，Cc—方解石，Chl—绿泥石，Pl—斜长石

Fig.3 Photomicrographs of the mafic rocks in Dahongshan

a−Pyroxenes altered into amphibole and chlorite locally, and plagioclases basically replaced by clay minerals in the gabbro in Guankouya (+); b−The diabasic structure in the diabase in Luojiaju, where pyroxene is basically replaced by chlorite (−); c−Almond texture of Changhe basalt, with the filling materials being mainly calcite (+); d−Pillow basalt of Changhe with intergranular texture (+); Am−Amphibole, Aug−Augite, Cc−Calcite, Chl−Chlorite, Pl−Plagioclase

加权平均年龄计算(Ludwig, 2003；杨绍等, 2018)。

4 岩石地球化学特征

大洪山地区镁铁质岩岩石手标本和镜下都可看到绿泥石化、碳酸盐化现象，其在后期构造改造、风化剥蚀过程中经历了一定程度的蚀变作用，这种蚀变对活动性元素有影响。因此，在进行相关解释和构造环境判别时，采用高场强元素(HFSE)Nb、Ta、Ti、Zr、Hf、Th和稀土元素(REE)等受蚀变作用影响较小的元素进行岩石分类、成因和形成环境的分析(Polat et al., 2003；Hastie et al., 2007;Pearce, 2014)。用于本文分析的地球化学数据除南风垭和姚家冲12件为实测外，其余六里冲、杨家棚、周家湾、厂河、花山共41件样品数据均选自前人研究成果。

六里冲辉长岩、南风垭玄武岩、杨家棚玄武岩和辉长岩、姚家冲玄武岩和辉绿岩、周家湾玄武岩、厂河枕状玄武岩、花山玄武岩具有比较一致的地球化学特征，认为其应为同一构造环境下的产物。大洪山地区镁铁质岩SiO_2含量为40.00%~54.45%，属于基性-中性岩范围，Na_2O含量为0.07%~5.96%，K_2O含量0.04%~4.15%，全碱(Na_2O+K_2O)含量为2.81%~6.05%，表现为亚碱性玄武岩系列的特点(Le Bas et al., 1986)，在Zr/Ti−Nb/Y图中，大洪山地区镁铁质岩样品基本落在亚碱性玄武岩范围内(图4a)。有着较高的Al_2O_3(12.49%~18.52%)、CaO(1.08%~11.28%，平均8.79%)、TiO_2(1.16%~3.55%)含量，MgO含量为3.61%~9.54%，全铁FeO^T含量8.79%~16.82%，FeO^T/MgO比值为0.99~3.47，在SiO_2−FeO^T/MgO图解中，整体落在拉斑玄武岩系列中(图4b)。少量样品SiO_2含量大于52%，且有着较高的MgO含量，但在既定的SiO_2含量下，同样相对较高的FeO^T含量和FeO^T/MgO比值使其区别于一般

表1 大洪山地区镁铁质岩主量元素(%)、微量元素和稀土元素(10^{-6})地球化学分析数据

Table 1 Mayor elements (%) and trace elements (10^{-6}) compositions of the mafic rocks in Dahongshan area

样号	D5017-2	D5017-4	D5017-9	D5018-4	D5019-2	D5020-2	D5021-4	PM02/10-2	PM02/13-1	PM02/15-1	D4021-7	D5071-1	分析精度
采样地点	姚家冲							南风垭					
岩性	辉长岩							玄武岩					
SiO_2	48.50	54.45	45.95	45.16	46.47	45.96	40.00	46.05	49.86	46.86	44.68	49.94	0.05
TiO_2	2.10	3.55	2.09	1.80	2.49	2.61	2.25	2.09	2.76	3.05	2.93	2.94	0.02
Al_2O_3	14.51	13.38	16.88	15.54	12.89	18.52	17.84	14.17	13.23	12.62	12.49	13.54	0.02
Fe_2O_3	3.75	9.76	2.09	3.25	6.42	3.45	3.32	4.00	4.68	5.38	6.58	4.48	0.02
FeO	6.00	2.80	8.40	7.35	7.30	10.15	12.25	8.25	9.45	8.55	7.6	8.75	0.02
MnO	0.12	0.01	0.10	0.17	0.16	0.10	0.14	0.10	0.04	0.20	0.26	0.09	0.02
MgO	3.61	4.81	7.19	4.14	3.77	4.44	6.88	6.40	8.90	6.25	3.90	6.81	0.02
CaO	6.93	1.31	4.06	8.21	7.23	2.61	4.07	5.49	1.08	5.66	7.53	2.66	0.02
Na_2O	2.45	0.77	3.68	2.27	3.06	3.25	2.40	2.90	2.05	2.69	3.34	0.07	0.02
K_2O	2.32	4.15	1.22	1.78	1.57	1.73	1.05	1.31	1.25	1.59	1.46	3.32	0.03
P_2O_5	0.39	0.82	0.35	0.42	0.46	0.46	0.40	0.28	0.64	0.32	0.56	0.75	0.02
LOI	8.26	3.73	6.83	8.96	7.18	5.41	8.16	7.87	4.85	5.70	7.66	5.52	0.02
$Mg^{\#}$	40.71	42.52	55.49	41.82	33.94	37.42	44.58	49.04	53.73	45.42	33.96	48.72	-
Sc	37.97	39.33	40.54	27.02	33.88	44.54	49.69	39.84	31.83	39.73	33.73	32.73	0.5
V	352	438	353	244	397	404	362	386	361	441	394	344	2
Cr	148.3	26.24	219.6	77.41	27.80	215.9	230.1	104.40	12.20	45.36	30.51	11.03	2
Co	45.92	58.40	65.35	34.91	41.77	71.79	48.40	46.98	38.20	41.72	31.08	28.81	0.04
Ni	68.86	45.98	77.39	19.44	15.90	61.79	65.40	47.10	13.25	23.80	16.04	6.77	1
Zn	119	151	181	103	129	152	184	155	123	126	-	145	1
Rb	36.57	69.15	17.90	30.28	22.14	19.04	17.50	30.56	25.68	27.78	24.19	64.81	3
Sr	160.9	25.42	107.3	343.0	194.3	56.95	55.44	30.56	25.68	27.78	24.19	64.81	2
Y	32.17	45.50	31.10	38.12	38.42	41.16	42.98	40.16	59.69	66.11	58.01	61.72	0.12
Nb	6.10	6.48	5.20	6.20	5.96	5.54	4.62	5.08	7.08	5.09	4.41	7.45	1.4
Zr	152	227	141	165	187	170	138	126	303	217	195	332	1.5
Ba	1832	176	563	532	272	150	144	211	191	275	200	168	5
Hf	3.65	4.45	3.56	4.01	4.36	3.74	2.85	3.03	6.68	4.81	5.50	6.59	0.1
Ta	0.57	0.50	0.47	0.62	0.49	0.52	0.51	0.60	0.49	0.40	0.35	0.50	0.1
Pb	4.23	4.10	3.83	5.15	7.00	6.67	3.37	10.02	10.40	12.60	7.22	4.77	0.2
Th	1.09	1.12	0.59	1.75	2.43	0.83	0.60	1.35	2.97	1.92	0.99	1.95	0.2
U	0.38	0.52	0.73	0.34	0.60	0.48	0.16	0.39	0.66	0.49	0.23	0.52	0.05
La	12.59	17.42	15.24	18.63	22.36	15.49	18.81	12.31	23.69	15.45	23.90	28.18	0.1
Ce	32.86	39.13	33.09	44.15	49.52	36.59	32.85	28.31	56.37	37.33	52.78	66.17	0.2
Pr	5.18	6.65	5.12	6.43	6.86	5.43	5.76	4.28	8.25	5.86	7.76	9.82	0.015
Nd	23.45	32.10	23.47	28.45	29.82	24.43	26.14	19.83	36.25	27.71	35.52	43.97	0.078
Sm	5.79	8.71	5.88	6.79	7.21	6.54	6.95	5.58	9.14	8.13	9.41	10.89	0.027
Eu	1.51	2.42	1.75	1.99	1.99	1.95	2.19	1.81	2.40	2.37	3.21	2.76	0.009
Gd	5.93	9.79	6.36	7.20	7.56	7.72	8.11	6.54	10.34	10.16	10.14	11.79	0.027
Tb	0.99	1.51	1.02	1.14	1.20	1.27	1.32	1.11	1.68	1.80	1.83	1.90	0.017
Dy	6.17	8.81	6.27	7.20	7.52	7.84	8.13	7.04	10.71	11.99	10.70	11.97	0.032
Ho	1.21	1.67	1.19	1.44	1.43	1.52	1.55	1.43	2.19	2.44	2.12	2.31	0.007
Er	3.36	4.35	3.10	3.99	4.10	4.31	4.22	4.06	6.28	7.04	5.86	6.42	0.031
Tm	0.45	0.55	0.40	0.56	0.58	0.59	0.56	0.57	0.90	0.99	0.89	0.88	0.007
Yb	2.60	3.28	2.28	3.32	3.38	3.59	3.24	3.35	5.33	5.76	5.54	5.21	0.031
Lu	0.38	0.44	0.34	0.51	0.51	0.54	0.49	0.49	0.79	0.85	0.79	0.74	0.005
ΣREE	102.47	136.83	105.51	131.82	144.02	117.80	120.31	96.71	174.34	137.88	170.45	203.02	-
LREE	81.39	106.43	84.55	106.44	117.75	90.43	92.69	72.12	136.11	96.85	132.58	161.80	-
HREE	21.08	30.39	20.95	25.38	26.26	27.37	27.62	24.58	38.24	41.03	37.87	41.23	-
LREE/HREE	3.86	3.50	4.04	4.19	4.48	3.30	3.36	2.93	3.56	2.36	3.50	3.92	-
$(La/Yb)_N$	3.48	3.81	4.79	4.02	4.75	3.09	4.17	2.63	3.19	1.92	3.09	3.88	-
δEu	0.73	0.75	0.81	0.80	0.76	0.78	0.83	0.85	0.70	0.74	0.93	0.69	-

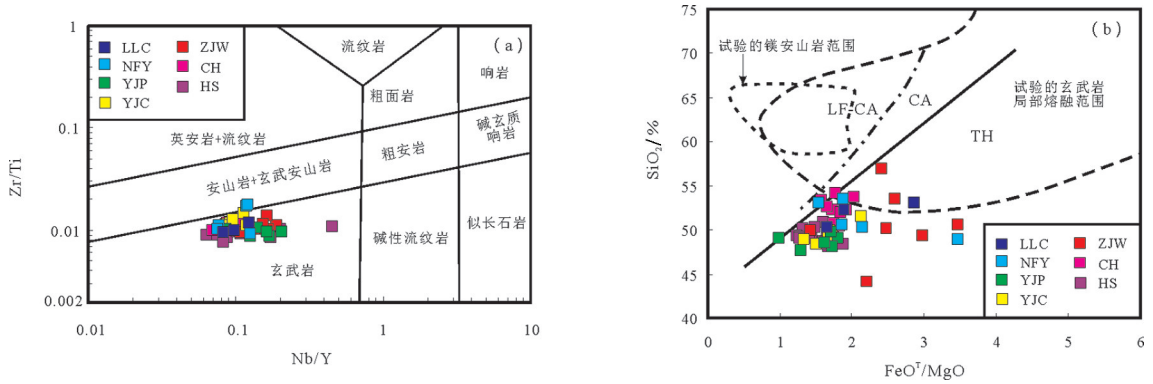

图4 大洪山镁铁质岩Nb/Y−Zr/Ti图(a)(底图据Pearce, 2014)和FeOT/MgO−SiO_2图(b)(底图据Miyashiro, 1974;邓晋福等, 2010)

LLC—六里冲辉长岩,数据来源于胡正祥等, 2015a;NFY—南风垭玄武岩;YJP—杨家棚玄武岩和辉长岩,数据来源于石玉若等, 2003, 2005b;YJC—姚家冲玄武岩和辉绿岩,ZJW—周家湾玄武岩,数据来源于董云鹏等, 2003;CH—厂河枕状玄武岩,数据来源于Deng et al., 2013;HS—花山玄武岩,数据来源于董云鹏等, 1999,后文图片中代号与此图一致

Fig.4 Nb/Y −Zr/Ti (a) (after Pearce, 2014) and FeO^T/MgO−SiO_2 diagram (b) (after Miyashiro, 1974; Deng Jinfu et al., 2010)of the mafic rocks in Dahongshan

LLC−Gabbros of Liulichong, data from Hu Zhengxiang et al., 2015a; NFY−Basalts of Nanfengya, YJP−Basalts and gabbros of Yangjiapeng, data from Shi Yuruo et al., 2003, 2005b; YJC−Basalts and diabases of Yangjiapeng, ZJW−Basalts of Zhoujiawan, data from Dong Yunpeng et al., 2003; CH−Pillow basalts of Changhe, data after Deng et al., 2013; HS−Basalts of Huashan, data from Dong et al., 1999. The Abbreviations in the figures below are coincident.

洋内弧(高)镁安山岩(邓晋福等, 2010)(图4b)。

大洪山地区镁铁质岩总稀土元素含量(ΣREE)为31.81×10^{-6}~203.02×10^{-6},平均87.35×10^{-6},有着较低ΣREE含量,但明显高出典型洋内弧高镁安山岩ΣREE含量(Mirdita高镁安山岩ΣREE平均含量7.19×10^{-6},马里亚纳高镁安山岩ΣREE平均含量8.77×10^{-6})。ΣLREE/ΣHREE比值为1.41~4.48,$(La/Yb)_N$=0.76~4.79(平均2.67),有着较低的轻、重稀土分异度,在球粒陨石标准化的稀土配分图上表现为平坦的配分模式(图5a)。δCe=0.75~1.39(平均0.99),基本无Ce异常,δEu=0.68~1.06(平均0.87),有轻微负Eu异常,说明存在斜长石的分离结晶。在N−MORB标准化微量元素蛛网图上(图5b),六里冲辉长岩、南风垭玄武岩、杨家棚玄武岩和辉长岩、姚家冲玄武岩和辉绿岩、周家湾玄武岩、厂河枕状玄武岩、花山玄武岩具有较为一致的配分模式。都富集大离子亲石元素(LILE)Rb、Ba、K、Pb和高场强元素(HFSE)Th、U,而亏损高场强元素Nb、Ta,而这类型的微量元素配分模

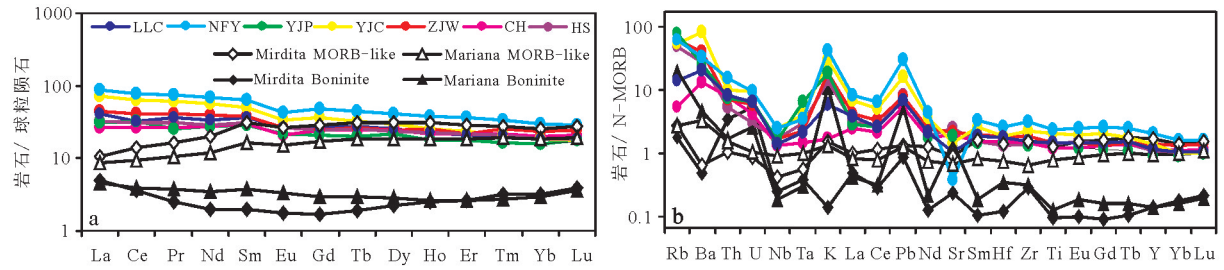

图5 大洪山地区镁铁质岩球粒陨石标准化REE配分图(a,Sun et al., 1989)和N−MORB标准化蛛网图(b,Ishizuka et al., 2009)

(图中均为平均值. Mirdita MORB−like和Mirdita Boninite分别代表阿尔卑斯−喜马拉雅造山带西段Mirdita地区的前弧玄武岩和高镁安山岩,数据来源于Dilek and Furnes, 2009a;Mariana MORB−like和Mariana Boninite分别代表西太平岩俯冲带马里亚纳前弧玄武岩和高镁安山岩,数据来源于Reagan et al., 2010)

Fig.5 Chondrite−normalized REE patterns (a, after Sun et al., 1989) and N−MORB−normalized spidergrams (b, after Ishizuka et al., 2009) of the mafic rocks in Dahongshan

(Data in the picture stand for average data. Data of Mirdita MORB−like basalt and Mirdita Boninite after Dilek and Furnes, 2009a;Mariana MORB−like basalt and Mariana Boninite after Reagan et al., 2010)

表2 南风垭、绿林寨玄武岩LA-ICP-MS锆石U-Pb测年数据

Table 2 LA-ICP-MS zircon U-Pb isotopic data of the basalt from Nanfengya and Lulinzhai

分析	含量/10^{-6}			Th/U	比值						年龄/Ma						谐和
点号	Pb	Th	U		$^{207}Pb/^{206}Pb$	1σ	$^{207}Pb/^{235}U$	1σ	$^{206}Pb/^{238}U$	1σ	$^{207}Pb/^{206}Pb$	1σ	$^{207}Pb/^{235}U$	1σ	$^{206}Pb/^{238}U$	1σ	度
PM02-15-1																	
1	50.7	998.9	732.8	1.36	0.0533	0.0015	0.3437	0.0098	0.0465	0.0006	343	95	300	7	293	3	97%
2	166	77.9	1262.3	0.06	0.0672	0.0015	1.1407	0.0362	0.1216	0.0019	856	51	773	17	740	11	95%
3	162.8	35.1	1159	0.03	0.0716	0.0015	1.2095	0.0263	0.1214	0.0011	976	43	805	12	739	6	91%
4	625.5	4263.8	8636.7	0.49	0.0564	0.0011	0.4606	0.0089	0.0587	0.0006	478	41	385	6	368	4	95%
5	84.5	406.4	453.6	0.9	0.0654	0.0018	1.2338	0.0345	0.1358	0.0017	787	56	816	16	821	10	99%
6	90.4	253.4	540.2	0.47	0.0663	0.0018	1.254	0.0345	0.1366	0.002	817	54	825	16	825	11	99%
7	74.8	959.9	1759	0.55	0.0513	0.002	0.2633	0.011	0.0372	0.0007	254	89	237	9	236	5	99%
8	219.5	36.4	1472	0.02	0.0631	0.0013	1.1812	0.0243	0.1345	0.0012	722	11	792	11	814	7	97%
9	109.9	431.3	633.3	0.68	0.0641	0.0015	1.1934	0.0274	0.1341	0.0012	743	48	798	13	811	7	98%
10	22.9	247.4	465.2	0.53	0.0596	0.0036	0.3224	0.0194	0.0411	0.0014	591	134	284	15	259	9	91%
11	78.1	991.3	1436.4	0.69	0.0636	0.0017	0.3609	0.01	0.0409	0.0005	728	25	313	7	258	3	80%
12	66.6	942.2	1167.1	0.81	0.0603	0.0017	0.3556	0.0104	0.0425	0.0005	617	61	309	8	268	3	85%
13	230.4	260.8	560.7	0.47	0.1168	0.0024	5.1845	0.1104	0.32	0.0035	1909	37	1850	18	1790	17	96%
14	28.8	294.1	577.8	0.51	0.0517	0.0022	0.2853	0.0119	0.0403	0.0006	272	98	255	9	255	4	99%
15	47	562	1014.2	0.55	0.0515	0.0018	0.2636	0.0091	0.0372	0.0005	261	75	238	7	235	3	99%
16	50.4	261.4	829.9	0.31	0.0546	0.0018	0.3891	0.0123	0.0518	0.0006	394	79	334	9	326	4	97%
17	631.6	1851.2	6441.6	0.29	0.0646	0.001	0.772	0.0153	0.0861	0.0013	761	33	581	9	532	7	91%
18	68.6	321.5	388.2	0.83	0.0687	0.0018	1.2832	0.0335	0.1362	0.002	900	54	838	15	823	11	98%
PM406-54-1																	
1	34.8	54.8	102.4	0.54	0.0561	0.0011	0.5564	0.0118	0.0719	0.0009	457	44	449	8	448	5	99%
2	281.1	424.5	366.2	1.16	0.0659	0.0007	1.0597	0.0135	0.1164	0.0009	1200	26	734	7	710	5	96%
3	41.2	43.7	73.9	0.59	0.0671	0.0023	1.2158	0.0284	0.1338	0.0023	843	77	808	13	809	13	99%
4	30.4	58.1	91.5	0.63	0.0569	0.0011	0.5894	0.0129	0.075	0.0009	500	79	470	8	466	5	99%
5	62.7	77.4	97.3	0.8	0.0654	0.0012	1.2018	0.0218	0.1335	0.0016	787	38	801	10	808	9	99%
6	442.6	251.4	355.5	0.71	0.116	0.0011	5.021	0.0498	0.3132	0.0024	1896	21	1823	8	1756	12	96%
7	37.1	43.2	69.4	0.62	0.0696	0.0013	1.2779	0.0233	0.1333	0.0014	917	45	836	10	807	8	96%
8	29.2	32.8	49.4	0.66	0.0677	0.0013	1.2487	0.0258	0.1334	0.0015	861	40	823	12	807	8	98%
9	56.5	235.4	638.2	0.37	0.0567	0.0015	0.2505	0.0069	0.0319	0.0003	480	59	227	6	202	2	88%
10	41.3	49.5	61.1	0.81	0.0678	0.0019	1.244	0.0353	0.1339	0.0028	861	-140	821	16	810	16	98%
11	40.6	99.3	163.1	0.61	0.0852	0.0026	0.5556	0.0173	0.0472	0.0007	1320	64	449	11	297	4	59%
12	37	33.8	47.1	0.72	0.0665	0.0049	1.2514	0.0653	0.1359	0.0019	833	156	824	29	821	11	99%
13	45.9	53.5	69.2	0.77	0.0664	0.0012	1.2506	0.0269	0.1362	0.0018	820	34	824	12	823	10	99%
14	56.3	74.3	82.8	0.9	0.0655	0.0012	1.2132	0.0204	0.1344	0.0014	791	39	807	9	813	8	99%
15	8	115.3	119.8	0.96	0.0609	0.0044	0.0586	0.004	0.0072	0.0001	639	157	58	4	46	1	77%
16	28.5	30.6	53.5	0.57	0.0667	0.0013	1.2376	0.0278	0.1344	0.0018	828	47	818	13	813	10	99%
17	29.7	34.4	51.3	0.67	0.0687	0.0015	1.2836	0.0291	0.1357	0.0019	900	78	838	13	820	11	97%
18	27.7	29.8	50.5	0.59	0.0674	0.0014	1.2657	0.0279	0.1366	0.0021	850	44	830	13	825	12	99%
19	16.1	101.7	370.9	0.27	0.061	0.0019	0.134	0.004	0.016	0.0002	639	67	128	4	102	1	77%
20	20.5	22.6	38.5	0.59	0.0662	0.0015	1.2152	0.0314	0.1332	0.0021	813	47	808	14	806	12	99%
21	25.7	22.9	55.2	0.41	0.0682	0.0033	1.2599	0.0409	0.1343	0.0018	876	100	828	18	812	10	98%
22	28.7	60.6	93.9	0.65	0.0507	0.0024	0.5048	0.012	0.0724	0.0008	228	114	415	8	451	5	91%
23	43.8	44.1	73.7	0.6	0.0693	0.0029	1.2593	0.038	0.1334	0.0022	909	86	828	17	807	13	97%
24	27	30.9	54.9	0.56	0.0675	0.0014	1.2505	0.0244	0.1347	0.0014	854	43	824	11	815	8	98%
25	28.6	30.9	52	0.59	0.0672	0.0015	1.2569	0.0305	0.136	0.0022	856	51	827	14	822	13	99%
26	42.8	256.5	803.9	0.32	0.0496	0.0007	0.1671	0.003	0.0244	0.0003	189	35	157	3	155	2	98%
27	87.5	658.9	784.9	0.84	0.0506	0.0008	0.158	0.0028	0.0226	0.0002	233	39	149	2	144	1	96%
28	28.5	30.4	63.7	0.48	0.0678	0.0015	1.2373	0.0288	0.1329	0.002	861	45	818	13	804	12	98%
29	53.1	188.5	294.8	0.64	0.0532	0.0009	0.3299	0.0055	0.045	0.0004	339	37	289	4	284	3	97%
30	38.6	43.1	58.1	0.74	0.07	0.004	1.296	0.0428	0.1351	0.0019	928	119	844	19	817	11	96%

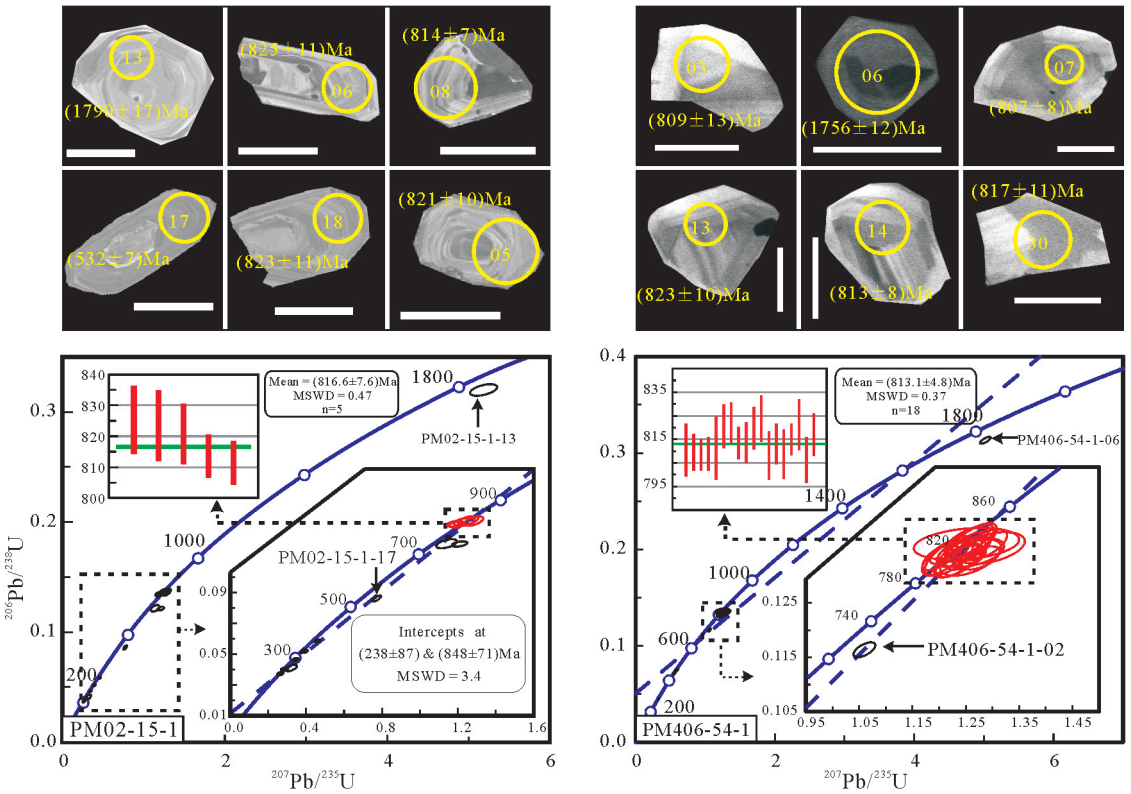

图6 南风垭、绿林寨玄武岩锆石阴极发光图和U-Pb年龄谐和图(白色短线代表50 μm)

Fig.6 Cathodoluminescence images and concordia plot for the basalt from Nanfengya and Lulinzhai (White bats in the figures stand for 50 μm)

式一般与俯冲相关的环境相联系。

5 LA-ICP-MS锆石U-Pb年龄

南风垭(PM02-15-1)、绿林寨(PM406-54-1)2件玄武岩测年样品中的锆石均呈自形-半自形短柱状,粒径整体较小,40~90μm不等,且整体而言,锆石振荡环带结构不明显,这些都符合玄武岩锆石结晶的特点(吴元保等, 2004),锆石U-Pb测年结果见表2和图6。

南风垭(PM02-15-1)玄武岩18个分析点中有2个分析点(No. 11、No. 12)谐和度小于90%,不参与年龄分析。其余16个分析点的Th含量35.1×10^{-6}~4263.8×10^{-6},U含量388.2×10^{-6}~8636.7×10^{-6},Th/U比值为0.02~1.36,整体表现为岩浆锆石的特点(吴元保等, 2004),但部分锆石从阴极发光图像和Th/U比值可以看出,其后期发生过一定程度的变质和Pb丢失。分析点No. 13锆石颗粒较大,与玄武岩结晶条件不符,$^{206}Pb/^{238}U$年龄为1790 Ma,应是岩浆上升过程中的捕获锆石。其余分析点形成的谐和图下交点238 Ma(误差较大),与秦岭—大别造山带广泛发育的印支构造事件时间基本一致(王清晨等, 2002; Liu et al., 2015)。上交点附近5个分析点较为集中,$^{206}Pb/^{238}U$加权平均年龄为(816.6±7.6) Ma (MSWD=0.47),代表南风垭玄武岩的形成年龄。

绿林寨(PM406-54-1)玄武岩30个分析点中有5个分析点(No. 09、No. 11、No. 15、No. 19、No. 22)因谐和度较低而舍弃。其余25个分析点的Th含量22.6×10^{-6}~658.9×10^{-6},U含量38.5×10^{-6}~803.9×10^{-6},Th/U比值在0.27~1.16,表现为岩浆锆石的特点(吴元保等, 2004)。分析点No. 06年龄为1756 Ma,应与南风垭玄武岩类似,同为岩浆上升过程中的捕获锆石。分析点No. 01、No. 04、No. 26、No. 27、No. 29年龄值分别为448 Ma、466 Ma、155 Ma、144 Ma、284 Ma,可能为锆石挑选过程中混入的年轻锆石,而分析点No. 02存在一定的Pb丢失,该6个分析点均不参与加权平均年龄计算。其余18个分析点在谐和图中较为集中,$^{206}Pb/^{238}U$加权平均年龄为(813.1±4.8) Ma (MSWD=0.37),代表绿林寨玄武岩的形成年龄。

6 讨 论

6.1 岩石成因

大洪山地区的镁铁质岩为一套拉斑玄武岩系列辉长(绿)岩-玄武岩组合,以岩块的形式混杂于一套碎屑岩基质中,具有典型造山带混杂岩的特点。高TiO_2、Al_2O_3、FeO^T,富集不相容元素、亏损高场强元素Nb、Ta的特点使之区别于正常洋中脊玄武岩(Sun et al., 1989);与典型俯冲带高镁安山岩(Boninite)相比,REE、Rb、Ba、Nb、Ta、Hf、Zr、Ti等微量元素几乎都高出一个数量级(Dilek et al., 2009b; Reagan et al., 2010)(图5);而相对较低的轻-重稀土分异度($\Sigma LREE/\Sigma HREE=1.41\sim4.48$)、Nb含量($1.66\times10^{-6}\sim13.31\times10^{-6}$,平均$4.27\times10^{-6}$)和Zr/Y比值(2.65~5.38,平均3.59)可区别于一般大陆溢流、裂谷玄武岩(严再飞等, 2010;Mattash et al., 2013)。大洪山镁

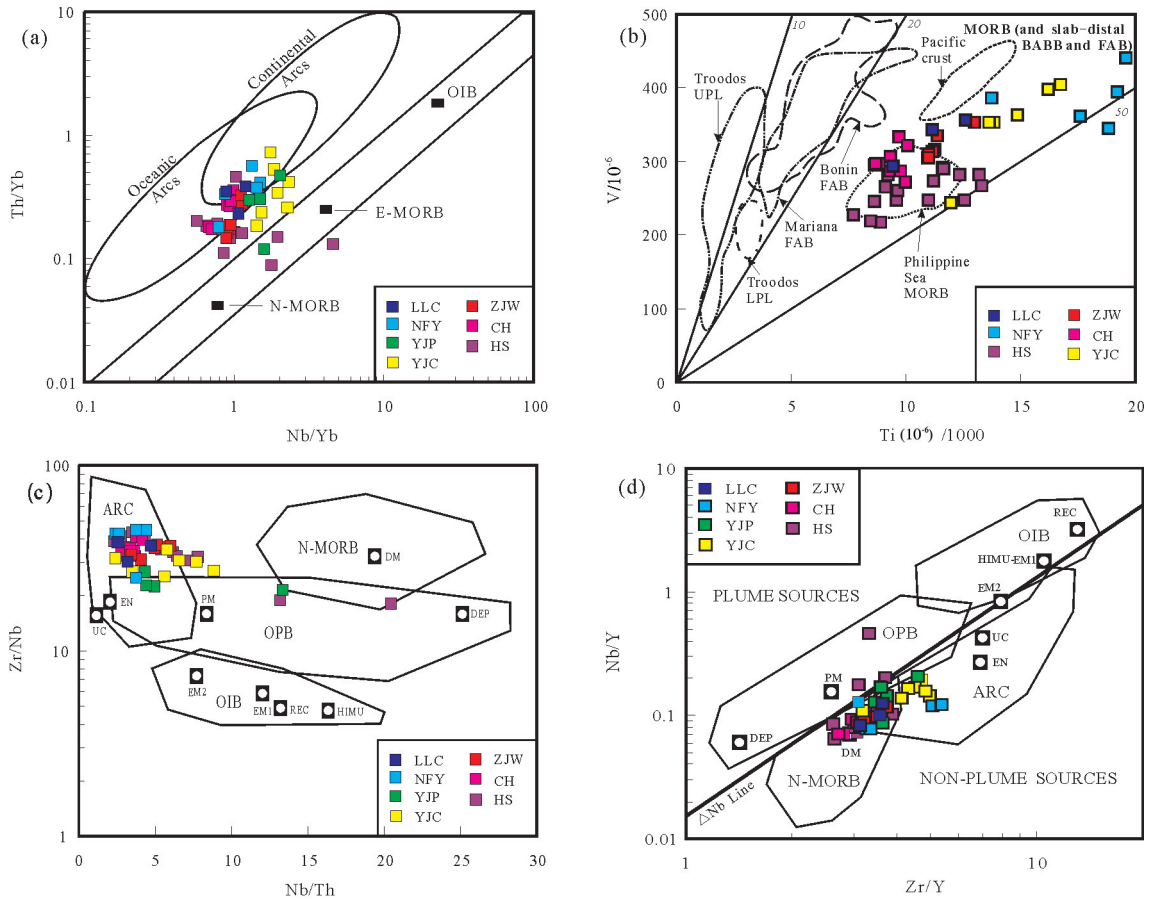

图7 大洪山地区镁铁质岩环境判别图解

a—Th/Yb – Nb/Yb图(Pearce, 2014);b—V-Ti/1000图(Shervais, 1982; Ishizuka et al., 2014a);c—Zr/Nb-Nb/Th图(Condie, 2003;Velásquez et al., 2011);d-Nb/Y-Zr/Y图(Fitton et al., 1997; Condie, 2003);Troodos UPL-塞浦路斯上部枕状熔岩;Troodos LPL-塞浦路斯下部枕状熔岩;Bonin FAB、Mariana FAB—小笠原、马里亚纳前弧玄武岩,Philippine Sea MORB-菲律宾海盆洋中脊玄武岩;Pacific crust-太平洋洋壳;ARC—与岛弧相关的玄武岩;N—MORB—正常洋中脊玄武岩;OIB—洋岛玄武岩;OPB—洋底高原玄武岩,DM—亏损地幔;EN—富集组分;PM—原始地幔;REC—循环组分;UC—大陆上地壳;DEP—亏损地幔组分;HIMU—高U/Pb比值的地幔;EM1、EM2—富集地幔

Fig.7 Tectonic discrimination diagram of the mafic rocks in the Dahongshan area

a-Th/Yb – Nb/Yb diagram (after Pearce, 2014), b-V – Ti/1000 diagram (after Shervais, 1982;Ishizuka et al., 2014a,)

c-Zr/Nb – Nb/Th diagram (after Condie, 2003;Velásquez et al., 2011), d-Nb/Y – Zr/Y diagram (after Fitton et al., 1997;Condie, 2003). Troodos UPL-Upper pillow basalt of Troodos;Troodos LPL-Lower pillow basalt of Troodos;Bonin FAB-Fore-arc basalt of Bonin, Mariana FAB-Fore-arc basalt of Mariana;Philippine Sea MORB- Mid- oceanic ridge basalt of Philippine Sea;ARC- Basalt associated with the island arc, N- MORB- Normal mid- ocean ridge basalt;OIB- Ocean island basalt, OPB- Ocean floor plateau basalt;DM- Depleted mantle;EN- Enriched components;PM- Primitive mantle;REC- Recirculated components;UC- Upper crust;DEP- Depleted mantle components;HIMU- High U/Pb ratio mantle;EM1, EM2-Enriched mantle 1, enriched mantle 2

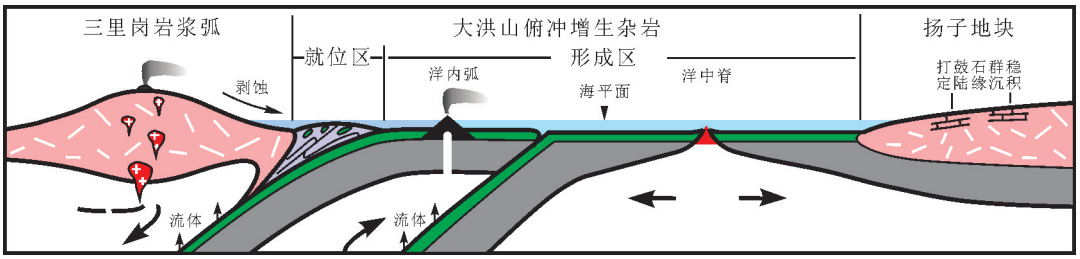

图8 大洪山镁铁质岩形成与就位模式图

Fig. 8 Formation process and emplacement mechanism of mafic rocks in Dahongshan

铁质岩Nb/Yb比0.56~4.59，Th/Yb比0.09~0.72，在Nb/Yb-Th/Yb图中，大部分样品投在与俯冲相关的洋内弧和大陆弧重叠且靠近洋内弧部位(图7a)；Ti/V比值为29.19~54.97，与一般Ti/V比小于20洋内弧岩石组合存在一定的差异，与菲律宾海盆中的洋中脊玄武岩有较大的重合(图7b)；样品Zr/Nb比17.90~44.59，Nb/Th比2.31~35.03(平均5.69)，在Zr/Nb-Nb/Th图中，主要表现为与俯冲相关的岛弧玄武岩相似(图7c)；而Nb/Y-Zr/Y图解中，样品整体投在与地幔柱无关的岛弧和正常洋中脊玄武岩重合部位(图7d)。

现代菲律宾海盆两侧同时发育两种不同的俯冲消减作用，其西侧为琉球-菲律宾洋-陆俯冲体系，发育典型的大陆边缘岛弧和弧后盆地(Savov et al., 2015)，而东侧为伊豆-小笠原-马里亚纳(IBM)洋内弧俯冲体系(Reagan et al., 2010; Ishizuka et al., 2014a, b)。对伊豆-小笠原-马里亚纳一带的洋内弧研究发现，其底部为洋壳性质的橄榄岩、辉长岩、辉绿岩，往上依次出现类洋中脊玄武岩(MORB-like)，又称其为前弧玄武岩(FAB)(肖庆辉等, 2016)、玻尼岩和高镁安山岩，再往上过渡到岛弧拉斑玄武岩系列和钙碱性系列的火山岩(Ishizuka et al., 2014a)，并且在阿尔卑斯—喜马拉雅造山带塞浦路斯(Cyprus)、欧曼(Oman)、土耳其Kizildag等经典蛇绿岩中发现了类似的岩石组合(Dilek et al., 2009a, b; Pearce et al., 2010; Goodenough et al., 2014)，洋内弧岩石序列及其地球化学特征均体现了正常洋盆向大陆边缘岛弧逐步演化的洋陆转换过程(邓晋福等, 2015)。洋内弧岩石组合中前弧玄武岩的出现是洋内初始俯冲开始的标志，其成岩岩浆由俯冲洋板片脱水交代亏损洋中脊地幔减压熔融产生，地球化学组成兼具亏损地幔源区的洋中脊玄武岩(MORB)和流体交代地幔源区的岛弧玄武岩(IAB)的共同特征，表现为二者过渡类型岩石组合的特点(Reagan et al., 2010; Ishizuka et al., 2014c; Pearce, 2014)。

大洪山地区土门—三里岗—小阜一带发育大量玄武岩-安山岩-英安岩-流纹岩组合(图1中Qbt)，其应为一套典型岛弧拉斑玄武岩系列到钙碱性系列火山岩(董云鹏等, 1999, 2003; 石玉若等, 2003)，且我们在酸性火山岩中已获得841 Ma、828 Ma的锆石U-Pb年龄(胡正祥等, 2015a, 2017)；加之三里岗中-酸性侵入岩具有岛弧TTG组合的特点，其形成时代为858~876 Ma(Shi et al., 2007; 廖明芳等, 2016; Xu et al., 2016)，二者应可以代表一个晋宁期的陆缘岩浆弧。本文研究的晋宁期镁铁质岩发育于该岩浆弧南侧，多以岩块的形式混杂在一套碎屑岩中，表现为造山带俯冲增生杂岩的特点(胡正祥等, 2015a, b)。且这些镁铁质岩岩块地球化学方面兼具岛弧玄武岩和洋中脊玄武岩的共同特点，其稀土配分模式和微量元素特征都与典型MORB-like玄武岩相似(图5)，我们推测大洪山镁铁质岩属于MORB-like玄武岩类岩石组合，其形成于洋内初始俯冲环境，成岩岩浆由俯冲洋板片脱水交代亏损洋中脊地幔减压熔融产生。

6.2 地质意义

在大洪山地区这套卷入混杂的镁铁质岩组合中，获得最老的可靠年代学证据为杨家棚辉长岩947 Ma(SHRIMP)(Shi et al., 2007)，其次为厂河枕状玄武岩中获得的824 Ma(SHRIMP)的年龄(Deng et al., 2013)，我们也曾经在厂河北绿林一带获得过辉绿岩820 Ma(LA-ICP-MS法)的证据(胡正祥等, 2015a)，加上本文中在南风垭、绿林寨分别获得的817 Ma、813 Ma玄武岩年龄，说明大洪山地区存在一套晋宁期(813~947 Ma)的镁铁质岩组合，它们形成于一种类似伊豆—小笠原—马里亚纳的洋内弧

初始俯冲环境,可能是该时间段内多期次洋内俯冲作用的产物。结合土门—三里岗—小阜一带弧火山-侵入岩的产出特点,我们推测晋宁期大洪山地区可能出现类似菲律宾海盆两侧洋内、洋陆两种俯冲作用同时并存的现象,南侧形成的洋内弧岩石组合最终呈残余岩块的形式构造就位于大陆边缘弧前增生楔中(图8)。这说明桐柏—大别地块与扬子地块之间晋宁期发生过一定规模的洋内-洋陆俯冲和造山运动,二者可能曾在青白口纪晚期拼合到一起。但美中不足的是,目前我们并未在大洪山地区发现确切的洋内俯冲作用相关的洋内弧(高)镁安山岩组合,也有可能该类岩石组合在漫长的地质演化中已经剥蚀殆尽。

7 结 论

(1)鄂北随州大洪山地区大量镁铁质岩以岩块的形式构造混杂在一套碎屑岩中,表现俯冲增生杂岩基质-岩块混杂的特点,这些镁铁质岩为拉斑玄武岩系列岩石组合,兼具岛弧玄武岩Nb、Ta亏损和洋中脊玄武岩REE低分异度的特点,与典型洋内弧MORB-like玄武岩相似,推测其形成于洋内初始俯冲环境,成岩岩浆由俯冲洋板片脱水交代亏损洋中脊地幔减压熔融产生。

(2)年代学方面,LA-ICP-MS锆石U-Pb测年分别获得南风垭、绿林寨玄武岩817 Ma、813 Ma的成岩年龄,结合已经取得的杨家棚辉长岩947 Ma、厂河枕状玄武岩824 Ma、绿林辉绿岩820 Ma的年龄结果,说明大洪山地区的这套前弧镁铁质岩组合大致形成于813~947 Ma,它们可能是多阶段洋内俯冲的产物。

(3)大洪山地区这套前弧镁铁质岩的厘定说明扬子地块与桐柏—大别地块之间晋宁期发生过一定规模的洋内-洋陆俯冲和造山运动,二者可能曾在青白口纪晚期拼合到一起。

致谢:感谢肖庆辉研究员、陆松年研究员、潘桂棠研究员等的技术指导,感谢彭练红教授、邓兴博士等的有益讨论,感谢审稿专家提出的建设性意见。

注释

❶湖北省地质局区域地质测量队. 1982. 1:20万宜城幅(H-49-V)、随县幅(H-49-M)区域地质调查报告[R]. 武汉: 湖北省地质调查院.

❷湖北省地质矿产局鄂东北地质大队一分队. 1986. 1:5万客店坡东半幅(H49-22-D)、古城畈幅(H49-23-C)、三阳店幅(H49-35-A)区域地质调查报告[R]. 武汉: 湖北省地质调查院.

References

Chen Chao, Mao Xinwu, Hu Zhengxiang, Yang Jinxiang, Yang Cheng, Kong Lingyao, Zheng Meng. 2017a. Discovery of ~817 Ma oceanic island basalts in the Dahongshan region, northern Hubei province and its significance[J]. Geological Science and Technology Information, 36(6): 22- 31(in Chinese with English abstract).

Chen Chao, Xiong Baocheng, Hu Zhengxiang, Zhou Feng, Yang Cheng, Kong Lingyao. 2017b. A rustic opinion of Neoproterozoic Ocean- continent coversion events on the northern margin of Yangtze Block[J]. Resources Environment & Engineering, 31(6): 1-14(in Chinese with English abstract).

Chen Chao, Yuan Jinling, Kong Lingyao, Ye Zhujun, Yang Qingxiong, Yang Cheng, Zhou Feng. 2018. Documentation of early Paleozoic Mafic Dykes in the Dahongshan region, northern Yangze block and its geological significance[J]. Earth Science, 43(7): 2370-2388(in Chinese with English abstract).

Condie Kent C. 2003. Incompatible element ratios in oceanic basalts and komatiites: Tracking deep mantle sources and continental growth rates with time[J]. Geochemistry, Geophysics, Geosystems, 4(1): 1-28.

Deng Jinfu, Feng Yanfang, Di Yongjun, Liu Cui, Xiao Qinghui, Su Shangguo, Zhao Guochun, Meng Fei, Ma Shuai, Yao Tu. 2015. Magmatic arc and ocean- continent transition: Discussion[J]. Geological Review, 61(3): 473- 484(in Chinese with English abstract).

Deng Jinfu, Liu Cui, Feng Yanfang. 2010. High magnesian andesitic/dioritic rocks (HMA) and magnesian andesitic/dioritic rocks (MA): Two igneous rock types related to oceanic subduction[J]. Geology in China, 37(4): 1112- 1118(in Chinese with English abstract).

Deng Qi, Wang Jian, Wang Zhengjiang, Wang Xuance, Qiu Yansheng, Yang Qingxiong, Du Qiuding, Cui Xiaozhuang, Zhou Xiaolin. 2013. Continental flood basalts of the Huashan Group, northern margin of the Yangtze block——Implications for the breakup of Rodinia[J]. International Geology Review, 55(15): 1865-1884.

Dilek Yildirim, Furnes Harald. 2009a. Structure and geochemistry of Tethyan ophiolites and their petrogenesis in subduction rollback systems[J]. Lithos, 113: 1-20.

Dilek Yildirim, Thy Peter. 2009b. Island arc tholeiite to boninitic melt evolution of the Cretaceous Kizildag (Turkey) ophiolite: Model for multi- stage early arc- forearc magmatism in Tethyan subduction factories[J]. Lithos, 113: 68-87.

Dong Yunpeng, Zhang Guowei, Liu Xiaoming, Lai Shaocong. 1998. Disintegration of the Huashan Group in the Dahongshan Mountain

Area, northern Hubei[J]. Regional Geology of China, 17(4): 371−376(in Chinese with English abstract).

Dong Yunpeng, Zhang Guowei, Lai Shaocong, Zhou Dingwu, Zhu Bingquan. 1999. An ophiolitic tectonic melange first discovered in Huashan area, south margin of Qinling Orogenic Belt, and its tectonic implications[J]. Science in China Series D: Earth Sciences, 43(3): 292−302.

Dong Yunpeng, Zhang Guowei, Lai Shaocong, Zhou Dingwu, Zhu Bingquan. 1999. An ophiolitic teconic melange first discovered in Huashan area, south margin of Qinling Orogenic Belt, and its tectonic implication[J]. Science in China (Series D), 29(3): 222−231(in Chinese with English abstract).

Dong Yunpeng, Zhang Guowei, Zhao Xia, Yao Anping, Liu Xiaoming. 2006. Geochemistry of the subduction−related magmatic rocks in the Dahong Mountains, northern Hubei Province[J]. Science in China Ser. D Earth Sciences, 47(4): 366−377.

Dong Yunpeng, Zhang Guowei, Zhao Xia, Yao Anping, Liu Xiaoming. 2003. Geochemistry and tectonic implication of igneous rocks in the northern Hubei Province: New evidence of subduction and eastward extension of the Mianlue ocean in the south Qinling[J]. Science of China (Series D), 33(12): 1143− 1153(in Chinese with English abstract).

Dong Yunpeng, Zhang Xiaoning, Liu Xiaoming, Li Wei, Chen Qing, Zhang Guowei, Zhang Hongfu, Yang Zhao, Sun Shengsi, Zhang Feifei. 2015. Propagation tectonics and multiple accretionary processes of the Qinling Orogen[J]. Journal of Asian Earth Sciences, 104: 84−98.

Fitton J G, Saunders A D, Norry M J, Hardarson B S, Taylor R N. 1997. Thermal and chemical structure of the Iceland plume[J]. Earth and Planetary Science Letters, 153: 197−208.

Goodenough Kathryn M, Thomas Robert J, Styles Michael T, Schofield David I, MacLeod Christopher J. 2014. Records of ocean growth and destruction in the Oman−UAE Ophiolite[J]. Elements, 10: 105−110.

Hastie A R, Kerr A C, Pearce J A, Mitchell S F. 2007. Classification of altered volcanic island arc rocks using immobile trace elements: Development of the Th−Co Discrimination Diagram[J]. Journal of Petrology, 48(12): 2341−2357.

Hu Zhengxiang, Chen Chao, Mao Xinwu, Deng Qianzhong, Yang Jinxiang, Li Linjing, Kong Lingyao. 2015a. Documentation of Jingningian Island−arc Volcanic Rocks and Accretionary complexes in the Dahongshan Region,Northern Hubei and Its tectonic Significance[J]. Resources Environment & Engineering, 29(6): 757−766(in Chinese with English abstract).

Hu Zhengxiang, Mao Xinwu, Tian Wangxue, Li Xiongwei. 2015b. Discovery of the Jinningian Orogenic Belt on the Northern Margin of Yangtze Craton in Mountain Dahong[J]. Geological Survey of China, 2(2): 33−39(in Chinese with English abstract).

Hu Zhengxiang, Chen Chao, Mao Xinwu, Yang Qingxiong, Deng Qianzhong, Kong Lingyao, Yang Cheng. 2017. The Qingbaikouan tumen formation−complex island arc volcanic−clastic rocks on the northern margin of yangtze block and its significance. Journal of Stratigraphy[J]. Journal of Stratigraphy, 41(3): 304−317(in Chinese with English abstract).

Ishizuka Osamu, Tani Kenichiro, Reagan Mark K. 2014a. Izu−Bonin−Mariana Forearc Crust as a Modern Ophiolite Analogue[J]. Elements, 10: 115−120.

Ishizuka Osamu, Geshi Nobuo, Kawanabe Yoshihisa, Ogitsu Itaru, Taylor Rex N, Tuzino Taqumi, Sakamoto Izumi, Arai Kohsaku, Nakano Shun. 2014b. Long− distance magma transport from arc volcanoes inferred from the submarine eruptive fissures offshore Izu− Oshima volcano, Izu− Bonin arc[J]. Journal of Volcanology and Geothermal Research, 285: 1−17.

Ishizuka Osamu, Umino Susumu, Taylor Rex N, Kanayama Kyoko. 2014c. Evidence for hydrothermal activity in the earliest stages of intraoceanic arc formation: Implications for ophiolite− hosted hydrothermal activity[J]. Society of Economic Geologists, Inc. Economic Geology, 109(8): 2159−2177.

Ishizuka Osamu, Yuasa Makoto, Taylor Rex N, Sakamoto Izumi. 2009. Two contrasting magmatic types coexist after the cessation of back−arc spreading[J]. Chemical Geology, 266: 274−296.

Lai Shaocong, Zhong Jianhua. 1999. Geochemical features and its tectonic significance of the meta− basalt in Zhoujiawan area, Mianlue suture zone, Qinling− Dabie mountains, Hubei province[J]. Scientia Geologica Sinica, 2(8): 127−136.

Le Bas M J, Le Maitre R W, Streckeisen A, Zanettin B. 1986. A chemical classification of volcanic rocks based on the total alkali−silica diagram[J]. Journal of Petrology, 27: 745−750.

Li Huaikun, Tian Hui, Zhou Hongying, Zhang Jian, Liu Huan, Geng Jianzhen, Ye Lijuan, Xiang Zhenqun, Ju Lesheng. 2016. Correlation between the Dagushi Group in the Dahongshan Area and the Shennongjia Group in the Shennongjia Area on the northern margin of the Yangtze Craton: Constraints from zircon U−Pb ages and Lu− Hf isotopic systematics[J]. Earth Science Frontiers, 23(6): 186−201(in Chinese with English abstract).

Liao Mingfang, Xie Yingbo, Li Linjing, Yang Jinxiang, Mao Xinwu, Deng Qianzhong, Kong Lingyao, Li Qiwen, Chen Chao. 2016. Discussion about genesis and formation age of Sanligang Pluton in the Dahongshan Region, Hubei[J]. Resources Enviroment & Engineering, 30(2): 143−150(in Chinese with English abstract).

Liu Xiaochun, Li Sanzhong, Jahn Bor−ming. 2015. Tectonic evolution of the Tongbai−Hong'an orogen in central China: From oceanic subduction/accretion to continent− continent collision[J]. Science China Earth Sciences, 58(9): 1477−1496.

Liu Yongsheng, Hu Zhaochu, Gao Shan, Günther Detlef, Xu Juan, Gao Changgui, Chen Haihong. 2008. In situ analysis of major and trace elements of anhydrous minerals by LA−ICP−MS without applying an internal standard[J]. Chemical Geology, 257: 34−43.

Lu Yuanfa. 2004. GeoKit− A geochemical toolkit for Microsoft Excel[J]. Geochimica, 33(5): 459− 464(in Chinese with English abstract).

Ludwig Kennethr. 2003. User's Manual for Isoplot 3.00: A Geochronological Toolkit for Microsoft Excel[M]. Berkeley: Berkeley Geochronology Center.

Ma Tianfang, Li Xiaoli, Chen Yongyun, Deng Zhenp, Li Guohui. 2011. Interchangeable Analysis of Method on the X− ray Fluorescence Spectrometry[J]. Rock and Mineral Analysis, 30(4): 486− 490(in Chinese with English abstract).

Mattash M A, Pinarelli L, Vaselli O, Minissale A, Al− Kadasi M, Shawki M N, Tassi F. 2013. Continental Flood Basalts and Rifting: Geochemistry of Cenozoic Yemen Volcanic Province[J]. International Journal of Geosciences, 4: 1459−1466.

Miyashiro Akiho. 1974. Volcanic rock series in island arcs and active continental margins[J]. American Journal of Science, 274: 321− 355.

Pearce J A, Robinson P T. 2010. The Troodos ophiolite complex probably formed in a subduction initiation, slab edge setting[J]. Gondwana Research, 18: 60−81.

Pearce J. A. 2014. Immobile Element fingerprinting of ophiolites[J]. Elements, 10: 101−108.

Polat A, Hofmann A. W. 2003. Alteration and geochemical patterns in the 3.7− 3.8 Ga Isua greenstone belt, West Greenland[J]. Precambrian Research, 126: 197−218.

Reagan Mark K, Ishizuka Osamu, Stern Robert J, Kelley Katherine A, Ohara Yasuhiko, Blichert− Toft Janne, Bloomer Sherman H, Cash Jennifer, Fryer Patricia, Hanan Barryb, Hickey− Vargas Rosemary, Ishii Teruaki, Kimura Jun− Ichi, Peate David W, Rowe Michael C, Woods Melinda. 2010. Fore− arc basalts and subduction initiation in the Izu− Bonin− Mariana system[J]. Geochemistry, Geophysics, Geosystems, 11(3): 10−1029.

Ren Jishun, Zhao Lei, Li Chong, Zhu Junbin, Xiao Liwei. 2017. Thinking on Chinese tectonics——Duty and responsibility of Chinese geologists[J]. Geology in China, 44(1): 33−43(in Chinese with English abstract).

Savov Ivanp, Ryan J G, D'Antonio M. 2015. Petrology and geochemistry of West Philippine basin Basalts and Early Palau− Kyushu arc volcanic clasts from ODP Leg 195, Site 1201D: Implications for the Early History of the Izu− Bonin− Mariana Arc[J]. Journal of Petrology, 47: 277−299.

Shervais John W. 1982. Ti− V plots and the petrogenesis of modern and ophiolitic lavas[J]. Earth and Planetary Science Letters, 59: 101−118.

Shi Yuruo, Zhang Zongqing, Liu Dunyi, Tang Suohan, Wang Jinhui. 2003. A study on Sm − Nd and Rb− Sr isotopic chronology of the Huashan ophiolitic Melange in the Suizhou Area，Hubei Province[J]. Geological Review, 49(4): 367− 373(in Chinese with English abstract).

Shi Yuruo, Zhang Zongqing, Liu Dunyi, Tang Suohan, Wang Jinhui, Chen Wen, Zhang Sihong, Liu Xinyu. 2005a. Rb− Sr and $^{40}Ar/^{39}Ar$ ages of the adamellite in Sanligang Area[J]. Acta Geoscientica Sinica, 26(1): 17−20(in Chinese with English abstract).

Shi Yuruo, Zhang Zongqing, Liu Dunyi, Tang Suohan, Wang Jinhui, Liu Tao. 2005b. Rb− Sr isotope dating of gabbro from Yangjiapeng Area in Suizhou, Hubei Province[J]. Acta Geoscientica Sinica, 26 (6): 521−524(in Chinese with English abstract).

Shi Yuruo, Liu Dunyi, Zhang Zongqing, Miao Laicheng, Zhang Fuqin, Xue Hongmei. 2007. SHRIMP zircon U− Pb dating of gabbro and granite from the Huashan ophiolite, oinling orogenic belt, China: Neoproterozoic suture on the northern margin of the Yangtze Craton[J]. Acta Geologica Sinica, 81(2): 239−243.

Sun S S, McDonough W F. 1989. Chemical and isotopic systematics of oceanic basalts: Implications for mantle composition and processes[J]. Geological Society, London, Special Publications, 42: 313−345.

Velásquez Germán, Béziat Didier, Salvi Stefano, Tosiani Tommaso, Debat Pierre. 2011. First occurrence of Paleoproterozoic oceanic plateau in the Guiana Shield: The gold− bearing El Callao Formation, Venezuela[J]. Precambrian Research, 186: 181−192.

Wang Qingchen, Lin Wei. 2002. Geodynamics of the Dabieshan collisional orogenic belt[J]. Earth Science Frontiers, 9(4): 257−265 (in Chinese with English abstract).

Wu Yuanbao, Zheng Yongfei. 2004. Genesis of zircon and its constraints on interpretation of U−Pb age[J]. Chinese Science Bulletin, 49(16): 1589−1604(in Chinese with English abstract).

Xiao Qinghui, Li Tingdong, Pan Guitang, Lu Songnian, Ding Xiaozhong, Deng Jinfu, Feng Yimin, Liu Yong, Kou Caihua, Yang Linlin. 2016. Petrologic ideas for identification of ocean−continent transition: Recognition of intra− oceanic arc and initial subduction[J]. Geology in China, 43(3): 721− 737(in Chinese with English abstract).

Xu Yang, Yang Kunguang, Polat Ali, Yang Zhenning. 2016. The− 860Ma mafic dikes and granitoids from the northern margin of the Yangtze Block, China: A record of oceanic subduction in the early Neoproterozoic[J]. Precambrian Research, 275: 310−331.

Yan Zaifei, Huang Zhilong, Chen Mi, Zhou Jiaxi, Zhao Zheng, Ding Wei. 2010. Two distinct mantle sources for high− Ti basalts in the Emeishan overfall basalt province[J]. Journal of Jilin University (Earth Science Edition), 40(6): 1311− 1322(in Chinese with English abstract).

Yang Shao, Li Dewei, Chen Guifan, Li Hualiang, Zhang Shuo, Zhou Tao. 2018. The discovery of the Wuluqiong magnetite deposit in Tibet and its geological characteristics[J]. Geology in China, 45(6): 1214−1227(in Chinese with English abstract).

Zhang Guowei, Dong Yunpeng, Lai Shaocong, Guo Anlin, Meng Qingren, Liu Shaofeng, Cheng Shunyou, Yao Aanping, Zhang Zongqing, Pei Xianzhi, Li Sanzhong. 2003. Mianlue tectonic zone

and Mianlue suture zone on southern margin of Qinling Dabie orogenic belt[J]. Science in China (Series D), 33(12): 1121-1135 (in Chinese with English abstract).

Zhang Guowei, Cheng Shunyou, Guo Anlin, Dong Yunpeng, Lai Shaocong, Yao Anping. 2004. Mianlue paleo- suture on the southern margin of the Central Orogenic System in Qinling-Dabie——with a discussion of the assembly of the main part of the continent of China[J]. Geological Bulletin of China, 23(9/10): 846-853(in Chinese with English abstract).

Zhang Zongqing, Zhang Guowei, Liu Dunyi, Wang Zongqi, Tang Suohan, Wang Jinhui. 2006. Isotopic Geochrology and Geochemistry of Ophiolites, Granites and Clastic Sedimentary Rocks in the Qinling Orogenic Belt[M]. Beijing: Geological Publishing House, 1-348(in Chinese with English abstract).

Zhou Liangliang, Wei Junqi, Wang Fang, Chou Xiumei. 2017. Optimizationof the working parameters of LA-ICP-MS and its application to zircon U-Pb dating[J]. Rock and Mineral Analysis, 36(04): 350-359(in Chinese with English abstract).

附中文参考文献

陈超, 毛新武, 胡正祥, 杨金香, 杨成, 孔令耀, 峥孟. 2017a. 鄂北大洪山地区~817Ma洋岛玄武岩的发现及意义[J]. 地质科技情报, 36(6): 22-31.

陈超, 熊保成, 胡正祥, 周峰, 杨成, 孔令耀. 2017b. 扬子北缘新元古代洋陆转换事件刍议[J]. 资源环境与工程, 31(6): 1-14.

陈超, 苑金玲, 孔令耀, 叶竹君, 杨青雄, 杨成, 周峰. 2018. 扬子北缘大洪山地区早古生代基性岩脉的厘定及其地质意义[J]. 地球科学, 43(7): 2370-2388.

邓晋福, 冯艳芳, 狄永军, 刘翠, 肖庆辉, 苏尚国, 赵国春, 孟斐, 马帅, 姚图. 2015. 岩浆弧火成岩构造组合与洋陆转换[J]. 地质论评, 61(3): 473-484.

邓晋福, 刘翠, 冯艳芳, 肖庆辉, 苏尚国, 赵国春, 孔维琼, 曹文燕. 2010. 高镁安山岩/闪长岩类(HMA)和镁安山岩/闪长岩类(MA): 与洋俯冲作用相关的两类典型的火成岩类[J]. 中国地质, 37(4): 1112-1118.

董云鹏, 张国伟, 赖绍聪, 周鼎武, 朱炳泉. 1999. 随州花山蛇绿构造混杂岩的厘定及其大地构造意义[J]. 中国科学(D辑), 29(3): 222-231.

董云鹏, 张国伟, 柳小明, 赖绍聪. 1998. 鄂北大洪山地区"花山群"的解体[J]. 中国区域地质, 17(4): 371-376.

董云鹏, 张国伟, 赵霞, 姚安平, 柳小明. 2003. 鄂北大洪山岩浆带地球化学及其构造意义——南秦岭勉略洋盆东延及其俯冲的新证据[J]. 中国科学(D辑), 33(12): 1143-1153.

胡正祥, 陈超, 毛新武, 邓乾忠, 杨金香, 李琳静, 孔令耀. 2015a. 鄂北大洪山晋宁期岛弧火山岩和增生杂岩的厘定及地质意义[J]. 资源环境与工程, 29(6): 757-766.

胡正祥, 毛新武, 田望学, 李雄伟. 2015b. 扬子陆块北缘大洪山地区发现晋宁期造山带[J]. 中国地质调查, 2(2): 33-39.

胡正祥, 陈超, 毛新武, 杨青雄, 邓乾忠, 孔令耀, 杨成. 2017. 扬子北缘青白口系土门岩组岛弧火山-碎屑岩的定义及意义[J]. 地层学杂志, 41(3): 304-317.

李怀坤, 田辉, 周红英, 张健, 刘欢, 耿建珍, 叶丽娟, 相振群, 瞿乐生. 2016. 扬子克拉通北缘大洪山地区打鼓石群与神农架地区神农架群的对比:锆石SHRIMP U-Pb年龄及Hf同位素证据[J]. 地学前缘, 23(6): 186-201.

廖明芳, 谢应波, 李琳静, 杨金香, 毛新武, 邓乾忠, 孔令耀, 李启文, 陈超. 2016. 湖北省大洪山地区三里岗岩体成因及时代探讨[J]. 资源环境与工程, 30(2): 143-150.

路远发. 2004. GeoKit: 一个用VBA构建的地球化学工具软件包[J]. 地球化学, 33(5): 459-464.

马天芳, 李小莉, 陈永君, 邓震平, 李国会. 2011. X射线荧光光谱分析方法的共享[J]. 岩矿测试, 30(4): 486-490.

任纪舜, 赵磊, 李崇, 朱俊宾, 肖黎微. 2017. 中国大地构造研究之思考——中国地质学家的责任与担当[J]. 中国地质, 44(1): 33-43.

石玉若, 张宗清, 刘敦一, 唐索寒, 王进辉. 2003. 湖北省随州花山蛇绿混杂岩Sm-Nd、Rb-Sr同位素年代研究[J]. 地质论评, 49(4): 367-373.

石玉若, 张宗清, 刘敦一, 唐索寒, 王进辉, 陈文, 张思红, 刘新宇. 2005a. 湖北省随州三里岗地区二长花岗岩Rb-Sr、$^{40}Ar/^{39}Ar$同位素年龄[J]. 地球学报, 26(1): 17-20.

石玉若, 张宗清, 刘敦一, 唐索寒, 王进辉, 刘涛. 2005b. 湖北省随州杨家棚地区辉长岩Rb-Sr同位素年龄[J]. 地球学报, 26(06): 521-524.

王清晨, 林伟. 2002. 大别山碰撞造山带的地球动力学[J]. 地学前缘, 9(4): 257-265.

吴元保, 郑永飞. 2004. 锆石成因矿物学研究及其对U-Pb年龄解释的制约[J]. 科学通报, 49(16): 1589-1604.

肖庆辉, 李廷栋, 潘桂棠, 陆松年, 丁孝忠, 邓晋福, 冯益民, 刘勇, 寇彩化, 杨琳琳. 2016. 识别洋陆转换的岩石学思路——洋内弧与初始俯冲的识别[J]. 中国地质, 43(3): 721-737.

严再飞, 黄智龙, 陈觅, 周家喜, 赵正, 丁伟. 2010. 峨眉山溢流玄武岩省高钛玄武岩的两种不同地幔源特征[J]. 吉林大学学报(地球科学版), 40(6): 1311-1322.

杨绍, 李德威, 陈桂凡, 李华亮, 张硕, 周涛. 2018. 西藏乌鲁穷含铜磁铁矿床的发现及地质特征[J]. 中国地质, 45(6): 1214-1227.

张国伟, 程顺有, 郭安林, 董云鹏, 赖绍聪, 姚安平. 2004. 秦岭-大别中央造山系南缘勉略古缝合带的再认识——兼论中国大陆主体的拼合[J]. 地质通报, 23(9/10): 846-853.

张国伟, 董云鹏, 赖绍聪, 郭安林, 孟庆任, 刘少峰, 程顺有, 姚安平, 张宗清, 裴先治,李三忠. 2003. 秦岭-大别造山带南缘勉略构造带与勉略缝合带[J]. 中国科学(D辑), 33(12): 1121-1135.

张宗清, 张国伟, 刘敦一, 王宗起, 唐索寒, 王进辉. 2006. 秦岭造山带蛇绿岩、花岗岩和碎屑沉积岩同位素年代学和地球化学[M]. 北京: 地质出版社, 1-348.

周亮亮, 魏均启, 王芳, 仇秀梅. 2017. LA-ICP-MS工作参数优化及在锆石U-Pb定年分析中的应用[J]. 岩矿测试, 36(4): 350-359.